Influence of Source Interference on the Directivity of Jet Mixing Noise

Ulf Michel *
DLR, German Aerospace Center, Berlin, 10623 Germany

A simple model is proposed for the description of the interference effects on the radiation of jet mixing noise. It is used to show analytically that many experimental observations in the acoustic far field of a jet can be explained with the acoustic analogy. This relates not only to the directivity of a static jet as was already shown by Lighthill, but also to the unexpectedly high noise radiation into the forward arc in flight. It also explains the experimental evidence that the peak frequency of a static jet is almost constant over a wide range of emission angles for a static jet and is subject to a Doppler frequency shift in flight. It is necessary to describe the turbulent flow quantities in the coordinate system fixed on the nozzle, in which the source quantities are stationary random and the limits of the source integral are stationary. An integral for the power-spectral density is derived, which includes the quadrupole and the dipole sources. Turbulence convection is considered through a phase angle of the cross-spectral density of the sources. The influence of source interference is expressed in terms of an interference integral which describes the sound radiation of one source volume element. In order to achieve analytic solutions for this integral, the radial extension of the jet is neglected and simple models are introduced for the decay of the coherence with increasing axial separation of the source positions. The decay is shown to have a large influence on the radiation, especially into the forward arc.

Nomenclature

a_0	sound speed in the ambience of the jet
D_f	Doppler factor
D_j	nozzle diameter
f	frequency
F_d	interference integral for dipole sources
F_q	interference integral for quadrupole sources
Ma_f	flight Mach number
p, p'	pressure fluctuation
p_0	atmospheric pressure in ambience
q	source term
q_{ij}	quadrupole source quantity
q_i	dipole source quantity
Q_q	quadrupole source term in acoustic far field
Q_d	dipole source term in acoustic far field
r	geometric distance between source and observer
r_e	emission (or wave-normal) distance between source and observer
t	time
t_r	retarded time
U_f	flight speed
U_i	velocity vector of flight stream
U_j	jet speed
U_j/a_0	acoustic Mach number of jet
V	integration volume of source region
V_c	integration volume of coherence region
W_{pp}	power-spectral density of pressure fluctuations
W_{qqc}	power-spectral density of source term Q_q in source position $y_i + \eta_i$
W_{qqs}	power-spectral density of source term Q_q in source position y_i
W_{qq}	cross-spectral density of source term Q_q
W_{dd}	cross-spectral density of source term Q_d
x_i	observer position
y_i	source position
γ_d	coherence of Q_d between two source positions
γ_q	coherence of Q_q between two source positions
θ	angle between source and observer
θ_e	emission (wave normal) angle
η_i	separation vector between two source positions
ψ_q	phase difference due to source motion of quadrupole sources
ψ_d	phase difference due to source motion of dipole sources
ψ_r	phase difference due to retarded time difference
ρ	density
ρ_0	density of ambient fluid
σ	jet stretching factor due to flight speed
$[\ldots]$	term evaluated at the retarded time

*Senior Scientist, DLR, German Aerospace Center, Institute of Propulsion Technology, Engine Acoustics Branch, Müller-Breslau-Str. 8, 10623 Berlin, Germany, Honorary Professor Aeroacoustics, BTU Cottbus, Germany, ulf.michel@dlr.de, Member AIAA and DGLR

I. Introduction

THE sound generated by a free jet when it mixes with the ambience is an important contribution to the total noise emission of jet powered transport aircraft and it is the dominating noise source of military combat aircraft. The theory for the underlying sound generation process was developed by Lighthill.[1,2] Ffowcs Williams[3] included the influence of a flight speed. Lighthill and Ffowcs Williams discussed the sound radiation problem in a coordinate system fixed on the moving frame of turbulent "eddies" which were considered to be the sources of sound. With assumptions on how the sources scale on mean flow quantities Lighthill concluded that the sound intensity of a jet at 90 degrees to the axis is proportional to eighth power of the acoustic Mach number U_j/a_0, where U_j is the jet speed and a_0 the speed of sound in the ambience of the flow. The theory explained why the sound pressure level in the far field of a jet is larger in the rear arc (in the direction of the jet's mean velocity vector) than in the forward arc.

However, other experimental findings could not be explained with these results, e.g., the deviations from the eighth power relation for low jet speeds and for hot jets, the additional noise generated by supersonic jets, and the unexpectedly high noise radiation into the forward arc when the aircraft is in flight. In addition, the frequencies found experimentally in the rear arc are not higher than in the forward arc as was expected from the assumption of moving sources (they are even lower) and the frequencies in flight are modified according to the Doppler frequency shift with respect to the motion of the nozzle. Both findings suggest that the sources have to be described in the coordinate system fixed on the nozzle.

Ribner[4] was first to use such a coordinate system in which the turbulence satisfies the mathematically important condition of stationary randomness. The motion of the sources was considered by the cross-correlation function of the source quantities. This approach was later applied by Michalke[5] in the frequency domain when he introduced a wave model to describe the turbulence in the jet. Michalke expanded the source region into azimuthal components[6] and discussed the influence of source coherence on the sound radiation.[7,8] This means that the sound radiation of instability waves with growing and decaying amplitudes was already considered in the 1970s, a work that is unfortunately not properly cited in most of the papers dealing with the sound radiation of jets. Michalke's approach was later extended by Michalke & Michel[9,10] to include the effects of flight speed and of density non-uniformities. Frequency spectra were discussed by Michel & Michalke.[11,12] It was shown by Michel[13] that broadband shock noise can also be described with this variant of the acoustic analogy. Broadband shock noise is the result of a special form of Mach wave radiation.

The nozzle-fixed coordinate system was also used by Tam & Auriault[14] in their semi-empirical theory for the prediction of jet mixing noise. This choice was one condition for their success in predicting the spectral shape of the far-field noise as function of emission angle.

This paper is written with the objective of providing a source model for the acoustic analogy in the coordinate system of the nozzle, which is used in experiments and numerical simulations. The source model includes the effects of source coherence. A proper modeling of the coherence and interference of the distributed source field of a jet is likely important, when the noise emission of aeroengines is analyzed with microphone arrays in the geometric near field of the engine. The cross-spectral density matrix of the microphones is influenced by the coherence in the source field of the jet and it is very likely that the source distribution cannot be determined correctly with a point source model that neglects the source coherence. Therefore, the development of a model for the source coherence and interference inside the jet flow appears to be very important.

In order to include the effects of flight speed, the convective Lighthill equation is used for the analysis. The derivation of the solution for the power-spectral density in the geometric far field is presented in detail, although it was previously presented by Michel & Michalke,[12] a publication that is not readily available.

II. Sound generation by free turbulence

A. Convective Lighthill equation

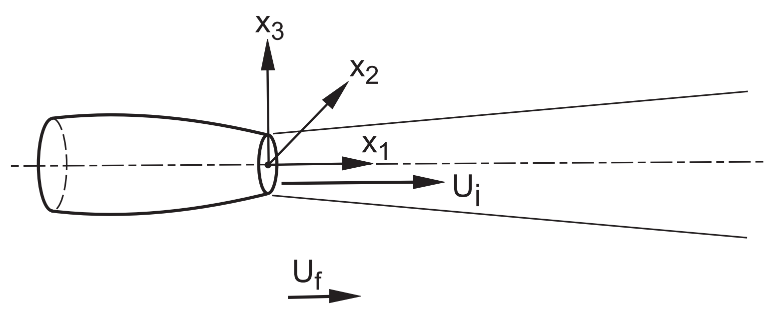

Figure 1. Turbulent jet with jet speed U_j as source of sound surrounded by a fluid with uniform flow speed U_f.

The situation of a jet in forward motion is shown in figure 1 in a coordinate system fixed on the nozzle. This coordinate system requires the use of the convective form of the Lighthill equation, which is given for the pressure p by

$$\frac{1}{a_0^2}\left(\frac{\partial}{\partial t}+U_i\frac{\partial}{\partial x_i}\right)^2 p-\frac{\partial^2 p}{\partial x_i^2}=q. \quad (1)$$

x_i describes the position relative to the nozzle center, U_i is the uniform flow velocity vector of the surrounding flow, and a_0 is the sound speed in the ambient flow. The source term q on the right hand side of equation (1) is given by (see Michalke & Michel[9])

$$q=\frac{\partial^2}{\partial x_i\partial x_j}\left(\rho u_i u_j-\tau_{ij}\right)-\left(\frac{\partial}{\partial t}+U_i\frac{\partial}{\partial x_i}\right)^2\left(\rho-\frac{p}{a_0^2}\right), \quad (2)$$

where $u_i=c_i-U_i$ is the difference between the local velocity c_i and the constant velocity U_i in the ambience. q is quadratically small outside the turbulent flow region. Equation (1) with $q=0$ describes the sound propagation in this space.

Eqs. (1) and (2) are exact because they are derived from the Navier-Stokes equations without restricting assumptions. If we assume that the entropy remains constant along streaklines, which means that the viscous dissipation and heat conduction have negligible influences on the sound generation, equation (2) can be approximated by

$$q=\frac{\partial^2 q_{ij}}{\partial x_i\partial x_j}+\frac{\partial q_i}{\partial x_i} \quad (3)$$

where the two terms q_{ij} and q_i are defined by

$$q_{ij}=\rho_o u_i u_j\left(1+\frac{p'}{\rho_o a_0^2}\right)-\left(1-\frac{\rho_o}{\rho}\right)p'\delta_{ij}, \quad (4)$$

and

$$q_i=p'\frac{\partial}{\partial x_i}\left(\frac{\rho_o}{\rho}\right). \quad (5)$$

$p'=p-p_0$ is the difference between the local pressure p inside the source region and the pressure p_0 in the ambience. a_0 is the speed of sound in the ambience. Terms of order $p'^2/\left(\rho_0 a_0^2\right)$ are neglected.

The first term on the right hand side of equation (3) describes a quadrupole source distribution because of the second spatial derivative of the tensor q_{ij}. This term yields the well known $(U_j/a_0)^8$ intensity relation of Lighthill[1,2] for the noise emission of a turbulent jet in a direction normal to the jet axis.

The second term on the right hand side of equation (3), the unsteady density source term, describes a dipole source distribution because of the first spatial derivative. The unsteady density source terms were discussed by Ffowcs Williams[15] but it was first shown by Morfey[16] that these terms may be important for hot jets. The unsteady density source term leads to a $(U_j/a_0)^6$ intensity relation (Michalke & Michel[10]) normal to the jet axis.

B. Solution of the convective Lighthill equation

1. Emission coordinates

The solution of the convective Lighthill equation (1) for the case of radiation into free space can be expressed in a very compact form as function of the emission (or wave-normal) angle θ_e and the emission distance r_e, which are defined in figure 2. $\theta_e=0$ is oriented in the flight direction. r_e is the wave-normal component of the distance between the source element $\mathrm{d}V(y_i)$ and the observer position. While the sound waves propagate from the source position to the observer, they are convected by a distance of $Ma_f r_e$ in the downstream direction, where $Ma_f=U_f/a_0$ is the flight Mach number.

The emission distance r_e and the emission angle θ_e can be computed from the geometric distance r and the observer angle θ as follows.

$$r_e=\frac{r}{\sqrt{1-Ma_f^2\sin^2\theta}-Ma_f\cos\theta} \quad (6)$$

and

$$\cos\theta_e=\cos\theta\left[\sqrt{1-Ma_f^2\sin^2\theta}-Ma_f\cos\theta\right]+Ma_f. \quad (7)$$

The inverse relations are

$$r=r_e\sqrt{1-2Ma_f\cos\theta_e+Ma_f^2} \quad (8)$$

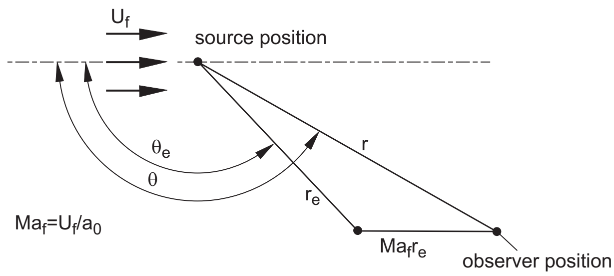

Figure 2. Relation between the source position and the observer position in a uniform flow (wind tunnel coordinate system).

and

$$\cos\theta = \frac{\cos\theta_e - Ma_f}{\sqrt{1 - 2Ma_f\cos\theta_e + Ma_f^2}}. \tag{9}$$

2. *Integral solution*

The solution for the sound pressure $p' = p - p_0$ in an observer position x_i is then given by the Kirchhoff integral (see Michalke & Michel[10]).

$$p'(x_i,t) = \frac{1}{4\pi}\int_V \frac{1}{r_e D_f}\left[\frac{\partial^2 q_{ij}}{\partial x_i \partial x_j}\right] \mathrm{d}V(y_i) + \frac{1}{4\pi}\int_V \frac{1}{r_e D_f}\left[\frac{\partial q_i}{\partial x_i}\right] \mathrm{d}V(y_i)\ . \tag{10}$$

The sound pressure is described by two integrals over the whole volume V that is occupied by the turbulent flow. The brackets in equation (10) indicate that the integrands have to be evaluated at the retarded time

$$t_r = t - r_e/a_0. \tag{11}$$

D_f is the Doppler factor, which is defined by

$$D_f = 1 - Ma_f\ \cos\theta_e. \tag{12}$$

equation (10) is valid everywhere in an unbounded space, even inside the turbulent flow.

3. *Acoustic far field*

The two source terms in equation (10) simplify in the acoustic far field of the sources, where the spatial derivatives can be replaced by time derivatives. This is shown by Michalke & Michel[10] for the convective wave equation.

$$\frac{\partial^2 q_{ij}}{\partial x_i \partial x_j} = \frac{1}{a_0^2 D_f^2}\frac{\partial^2 q_q}{\partial t^2} \tag{13}$$

$$\frac{\partial q_i}{\partial x_i} = \frac{1}{a_0 D_f}\frac{\partial q_d}{\partial t} \tag{14}$$

The influence of the Doppler factor D_f increases the source intensity against the flow direction ($\theta_e < 90°$), the increase being larger for the quadrupole sources q_q than for the dipole sources q_d.

The new source quantities q_q and q_d are defined by (Michalke & Michel[10])

$$q_q(y_i,\theta_e,t) = \rho_0 u_{r_e}^2\left(1 + \frac{p'}{\rho_0 a_0^2}\right) - \left(1 - \frac{\rho_0}{\rho}\right)p', \tag{15}$$

$$q_d(y_i,\theta_e,t) = p'\frac{\partial}{\partial y_{r_e}}\left(\frac{\rho_0}{\rho}\right). \tag{16}$$

For small values p' within the source region and for $\rho \approx \rho_0$ equation (15) can be approximated by

$$q_q \approx \rho_0 u_{re}^2. \tag{17}$$

The quadrupole source strength is dominated by the second time derivative of the square of the velocity fluctuations in the volume element d$V(y_i)$ in the direction θ_e toward the observer position x_i.

The dipole source strength is determined by the product of the first time derivative of the local pressure fluctuations p' und the derivative of the inverse of the density gradient in the direction θ_e toward the observer position x_i.

The solution for the sound pressure $p' = p - p_0$ in an observer position x_i in the acoustic far field and in free space is then given by (see Michalke & Michel[10]).

$$p'(x_i, t) = \frac{1}{4\pi a_0^2} \int\limits_V \frac{[Q_q]}{r_e {D_f}^3} \, \mathrm{d}V(y_i) + \frac{1}{4\pi a_0} \int\limits_V \frac{[Q_d]}{r_e {D_f}^2} \, \mathrm{d}V(y_i). \tag{18}$$

The quadrupole source term Q_q and the dipole source term Q_d in equation (18) are abbreviations for

$$Q_q(y_i, \theta_e, t) = \frac{\partial^2 q_q(y_i, \theta_e, t)}{\partial t^2} \tag{19}$$

$$Q_d(y_i, \theta_e, t) = \frac{\partial q_d(y_i, \theta_e, t)}{\partial t} \tag{20}$$

C. Time averaged solutions

1. Power-spectral density

One is generally not interested in the time-dependent solution for the sound pressure (like equation (18)) but in time averaged quantities. The power-spectral density function is studied here because it is required for the description of the important interference effects in the geometric far field of distributed sources.

The power-spectral density $W_{pp}(x_i, f)$ of the pressure fluctuations in the observer position x_i as function of the frequency f in the coordinate system of the nozzle is given by

$$W_{pp}(x_i, f) = W_{ppqq}(x_i, f) + W_{ppdd}(x_i, f). \tag{21}$$

It has contributions from the two source terms Q_q and Q_d, which are assumed to be uncorrelated.

2. Quadrupole noise

The power-spectral density $W_{ppqq}(x_i, f)$ of the pressure fluctuations due to the quadrupole source term Q_q in the acoustic far field is given by the double integral

$$W_{ppqq}(x_i, f) = \frac{1}{(4\pi a_0^2)^2} \int\limits_V \frac{1}{r_e D_f^3} \int\limits_{V_c} \frac{1}{r_{ec} D_{fc}^3} Re\{W_{qq}(y_i, y_{ci}, f) \exp(i\psi_r)\} \, \mathrm{d}V_c(y_{ci}) \, \mathrm{d}V(y_i) \tag{22}$$

with the cross-spectral density W_{qq} of the source term Q_q between the two positions y_i and $y_{ci} = y_i + \eta_i$, where η_i is the separation vector between the two volume elements.

$$W_{qq}(y_i, \eta_i, f) = \int\limits_{-\infty}^{\infty} \overline{Q_q(y_i, t) Q_q(y_i + \eta_i, t + \tau)} \exp(i2\pi f \tau) \, \mathrm{d}\tau, \tag{23}$$

Q_q is defined by equation (19). $Re\{\dots\}$ means *real part of.* r_e and D_f are the emission (wave-normal) distance and Doppler factor of the volume element d$V(y_i)$, respectively, and r_{ec} and D_{fc} are the corresponding values for the volume element d$V_c(y_i)$.

The influence of the emission distance r_e on the retarded times is considered in equation (22) through the phase difference ψ_r, which is given by

$$\psi_r = 2\pi f \frac{r_e - r_{ec}}{a_0} = k(r_e - r_{ec}), \tag{24}$$

where $k = 2\pi f / a_0$ is the wave number.

The cross-spectral density W_{qq} depends on the source positions y_i and $y_{ci} = y_i + \eta_i$ of the two volume elements d$V_c(y_{ci})$ and d$V(y_i)$, on the frequency f, the emission angles θ_e and θ_{ec} in the two source positions and all other parameters that influence the turbulence in the flow. Since the cross-spectral density is a complex quantity it can be expressed in terms of its amplitude and phase as follows

$$W_{qq} = |W_{qq}(y_i, y_{ci})| \exp(i\,\psi_q) \tag{25}$$

$$= \sqrt{W_{qq}(y_i, y_i)\, W_{qq}(y_{ci}, y_{ci})}\, \gamma_q(y_i, y_{ci}) \exp(i\,\psi_q) \tag{26}$$

The phase difference ψ_q is related to the phase speed of the disturbances in the jet's turbulence, which in turn is the result of turbulence convection. γ_q is the coherence of the source terms Q_q between the two source positions y_i and y_{ci}.

Eqs. (22), (24), and (26) are valid in the acoustic far field of the sources, but the observer position may be located in the geometric near field of the jet.

Equation (22) may be abbreviated as follows

$$W_{ppqq}(x_i, f) = \frac{1}{(4\pi a_0^2)^2} \underbrace{\int\limits_V \frac{W_{qqs}}{r_e^2 D_f^6} F_q \, \mathrm{d}V(y_i)}_{\text{integral over source volume}} \; . \tag{27}$$

with the abbreviation for the inner integral

$$F_q = \underbrace{\int\limits_{V_c} \underbrace{\frac{r_e D_f^3}{r_{ec} D_{fc}^3}}_{\text{convect.ampl.}} \underbrace{\sqrt{\frac{W_{qqc}}{W_{qqs}}}}_{\text{source strength}} \underbrace{\gamma_q}_{\text{coherence}} \underbrace{\cos(\psi_q + \psi_r)}_{\text{source interference}} \mathrm{d}V_c(\eta_i)}_{\text{integral over coherence volume}}, \tag{28}$$

$W_{qqs} = W_{qq}(y_i, y_i, f, \theta_e)$ is the power-spectral density of Q_q in the source position y_i and $W_{qqc} = W_{qq}(y_{ci}, y_{ci}, f, \theta_{ec})$ is the corresponding value in the second position $y_{ci} = y_i + \eta_i$. Both values describe the strength of the source term Q_q as function of the frequency f and emission angle θ_e in the two source positions. W_{qqc}/W_{qqs} is the relative source strength, where the source strength in position $y_i + \eta_i$ is normalized with the strength in position y_i. F_q is a normalized contribution of one source element $\mathrm{d}V(y_i)$ to the far field of the jet. It describes the interference effects between the power-spectral density W_{qqs} in the source element $\mathrm{d}V(y_i)$ and its complete neighborhood. γ_q indicates that only the coherent part of the fluctuations in the two positions contributes to the sound in the far field. The integration over the coordinate $\eta_i = y_{ci} - y_i$ in equation (28) needs only to be carried out over the region in which the coherence γ_q is not negligible. This region is termed coherence volume in the corresponding under-brace of equation (28).

The source interference term in equation (28) describes the phase relationship between the contributions from different source positions. The phase ψ_q considers the effect of source convection in the flow. ψ_r considers the influence of the difference of the retarded times between the two source positions and is defined by equation (24).

The product of coherence function times source interference function can have very large effects on the sound radiation of the source field and explains many features of the directivity of jet mixing noise. It will later be shown that this includes broadband shocknoise.

3. *Dipole noise*

The power-spectral density in equation (21) due to dipole noise is defined correspondingly.

$$W_{ppdd}(x_i, f) = \frac{1}{(4\pi a_0^2)^2} \underbrace{\int\limits_V \frac{W_{dds}}{r_e^2 D_f^4} F_d \, \mathrm{d}V(y_i)}_{\text{integral over source volume}} \tag{29}$$

with

$$F_d = \underbrace{\int\limits_{V_c} \underbrace{\frac{r_e D_f^2}{r_{ec} D_{fc}^2}}_{\text{convect.ampl.}} \underbrace{\sqrt{\frac{W_{ddc}}{W_{dds}}}}_{\text{source strength}} \underbrace{\gamma_d}_{\text{coherence}} \underbrace{\cos(\psi_d + \psi_r)}_{\text{source interference}} \mathrm{d}V_c(\eta_i)}_{\text{integral over coherence volume}}, \tag{30}$$

where W_{dds} and W_{ddc} are the power-spectral densities of the dipole source function Q_d (equation (20)) in the source volume elements $\mathrm{d}V(y_i)$ and $\mathrm{d}V_c(\eta_i)$, respectively. Note that the exponent of the Doppler factor D_f is only 4 in equation (29) rather than 6 in equation (27). The consequence for flyover results is that the forward arc radiation will be more dominated by quadrupole noise than the rear arc and that the flight effects are larger for jets with constant density than for heated jets.

4. *Geometric far field*

Eqs. (28) and (30) simplify if it is assumed that the observer position is located in the geometric far field of the coherence volume. The ratio $(r_e D_f^2)/(r_{ec} D_{fc}^2) \approx 1$. If it is further assumed that the source strength is almost constant within the coherence volume, we obtain

$$F_q = \underbrace{\int_{V_c} \underbrace{\gamma_q}_{\text{coherence}} \underbrace{\cos(\psi_q + \psi_r)}_{\text{source interference}} \, \mathrm{d}V_c(\eta_i)}_{\text{integral over coherence volume}}, \tag{31}$$

$$F_d = \underbrace{\int_{V_c} \underbrace{\gamma_d}_{\text{coherence}} \underbrace{\cos(\psi_d + \psi_r)}_{\text{source interference}} \, \mathrm{d}V_c(\eta_i)}_{\text{integral over coherence volume}}, \tag{32}$$

The influence of the retarded time difference on the phase difference ψ_r simplifies to

$$\psi_r = 2\pi f \Delta t_r = 2\pi f \frac{\eta_{r_e}}{a_0 D_f} = k \frac{\eta_{re}}{D_f}, \tag{33}$$

where η_{r_e} is the component in wave normal direction θ_e of the difference vector η_i between the two source volume elements $\mathrm{d}V_c$ and $\mathrm{d}V$ as illustrated in figure 3.

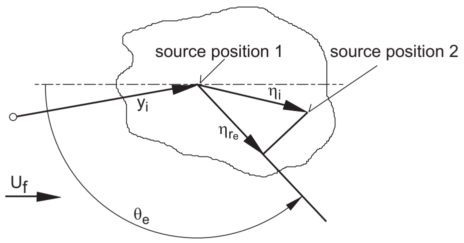

Figure 3. Definition of the vector η_i which describes the difference between the two source volume elements and of its component η_{r_e} in the wave normal direction.

5. *Normalization of equations*

With the nozzle diameter D_j as reference length, $\Delta U_j = U_j - U_f$ as reference speed, $D_j/\Delta U_j$ as reference time the quadrupole source term Q_q of equation (19) can be made dimensionless.

$$Q_q(y_i, x_i, t) = Q_q^\star(y_i, x_i, t) \frac{\rho_0 \, \Delta U_j^2}{(D_j/\Delta U_j)^2} = Q_q^\star(y_i, x_i, t) \frac{\rho_0 \, \Delta U_j^4}{D_j^2}, \tag{34}$$

where the star indicates a nondimensional quantity, which will be assumed independent of U_j, U_f, D_j, ρ_j in a first order approximation.

Michel & Michalke[9] considered the lengthening of the jet flow field in first order by introducing a jet stretching factor due to flight speed.

$$\sigma = 1 + A U_f/(U_j - U_f), \qquad A = 1.5 \tag{35}$$

This yields

$$\mathrm{d}V = \mathrm{d}V^\star \sigma D_j^3, \tag{36}$$

$$\mathrm{d}V_c = \mathrm{d}V_c^\star \sigma D_j^3, \tag{37}$$

$$F_q = F_q^\star \sigma D_j^3, \tag{38}$$

where $V^\star$ and $V_c^\star$ are the normalized source and coherence volumes and $F_q^\star$ the interference integral of the static jet.

This stretching was theoretically verified by an instability theory of Michalke & Hermann.[17] They also showed that the normalized frequency of the instability waves in the shear layer is increased in flight, yielding

$$f = f^\star \frac{\Delta U_j}{D_j} \sigma. \tag{39}$$

where $f^\star$ is the normalized frequency of the static jet.

The cross-spectral density of the source term Q_q in the source position y_i is then given by

$$W_{qqs} = \frac{\rho_0^2 \Delta U_j^7}{\sigma D_j^3} W_{qqs}^{\star 2}. \tag{40}$$

With $a_0^2 = \gamma p_0/\rho_0$ (γ is the isentropic exponent) we finally obtain

$$W_{ppqq} = \left(\frac{\gamma p_0}{4\pi}\right)^2 \left(\frac{D_j}{r_e}\right)^2 \left(\frac{\Delta U_j}{a_0}\right)^7 \frac{\sigma}{D_f^6} \int\limits_V W_{qqs}^\star F_q^\star \, \mathrm{d}V^\star(y_i), \tag{41}$$

where the nondimensional interference integral $F_q^\star$ is defined by

$$F_q^\star = \int\limits_{V_c^\star} \gamma_q \, \cos(\psi_q + \psi_r) \, \mathrm{d}V_c^\star(\eta_i), \tag{42}$$

Integration over the whole frequency range $(0, f_{\text{max}}^\star)$ yields for the quadrupole noise

$$\overline{p_q^2} = \left(\frac{\gamma p_0}{4\pi}\right)^2 \left(\frac{D_j}{r_e}\right)^2 \left(\frac{\Delta U_j}{a_0}\right)^8 \frac{\sigma^2}{D_f^6} \int\limits_V \int\limits_0^{f_{\text{max}}^\star} W_{qqs}^\star F_q^\star \, \mathrm{d}f^\star \mathrm{d}V^\star(y_i). \tag{43}$$

Corresponding results for the dipole noise are

$$W_{ppdd} = \left(\frac{\gamma p_0}{4\pi}\right)^2 \left(\frac{D_j}{r_e}\right)^2 \left(\frac{\Delta U_j}{a_0}\right)^5 \frac{\sigma}{D_f^4} \int\limits_V W_{dds}^\star F_d^\star \, \mathrm{d}V^\star(y_i), \tag{44}$$

$$F_d^\star = \int\limits_{V_c^\star} \gamma_d \, \cos(\psi_d + \psi_r) \, \mathrm{d}V_c^\star(\eta_i), \tag{45}$$

$$\overline{p_d^2} = \left(\frac{\gamma p_0}{4\pi}\right)^2 \left(\frac{D_j}{r_e}\right)^2 \left(\frac{\Delta U_j}{a_0}\right)^6 \frac{\sigma^2}{D_f^4} \int\limits_V \int\limits_0^{f_{\text{max}}^\star} W_{dds}^\star F_d^\star \, \mathrm{d}f^\star \mathrm{d}V^\star(y_i). \tag{46}$$

6. Interference as possible cause of directivity

An inspection of equations (43) or (46) shows that a directivity pattern of jet noise can have various origins. The Doppler amplification due to the Doppler factor D_f appears only in the flight condition. The directivity of a static jet can be caused by directivities of the power-spectral densities $W_{qqs}^\star$ or $W_{dds}^\star$, and by a directivity of the interference functions $F_q^\star$ or $F_d^\star$. The latter depend according to equations (42) and (45) on γ_q or γ_d, or on source interference effects caused by the terms $\cos(\psi_q + \psi_r)$ or $\cos(\psi_d + \psi_r)$. It will be shown, that many features of the directivity of jet noise can be explained with source interference effects.

It may be noted that the products $W_{qqs}^\star F_q^\star$ and $W_{dds}^\star F_d^\star$ must be independent of the chosen source description. Other source descriptions were proposed for low Mach number flows by Ribner[18] (pseudo-sound) and Powell[19] (vorticity) or the modifications by Möhring[20] and Obermeier.[21] Although the sources are different as was pointed out by Tam[22] the product of source spectral density times interference integral must yield the same result except for the influence of the simplifications. Different numerical values of W_{qqs} must be compensated by the corresponding values of F_q.

III. Analytical solutions with simple source model

A. Line model for jet

Simplifications are required to make possible analytical solutions of the equations (31) and (32).

In a first step, the radial extension of the source volume is neglected. This is a drastic simplification since the far field of the jet becomes axisymmetric in contrast to experimental evidence of Maestrello.[23] Nevertheless, we will see that major features of the directivity can be explained with this simple assumption.

The line model allows to simplify the distance η_{r_e} in equation (33) by

$$\eta_{r_e} = \eta_1 \cos\theta_e, \tag{47}$$

which yields

$$\psi_r = k\eta_1 \frac{\cos\theta_e}{D_f}, \tag{48}$$

The phase difference ψ_q is caused by the convection of the turbulence in the shear layer of the jet. The phase difference between two source positions separated in the axial direction by η_1 may be approximated by a relation derived from the wave propagation of instability waves,

$$\psi_q = 2\pi f \frac{\eta_1}{U_p(f, y_i, \eta_i)} = k\eta_1 \frac{a_0}{U_p(f, y_i, \eta_i)}. \tag{49}$$

$U_p(f, y_i, \eta_i)$ is the average phase velocity in the η_1-direction of the considered frequency component between positions y_i and $y_i + \eta_i$. The phase angle $\psi = \psi_q + \psi_r$ in the interference function of equation (31) is then given by equations (48) and (49),

$$\psi = \psi_q + \psi_r = k\,\eta_1 \left(\frac{a_0}{U_p} + \frac{\cos\theta_e}{D_f} \right). \tag{50}$$

If we introduce a coherence length scale of the quadrupole sources

$$L_{xq} = \int_{-\infty}^{\infty} \gamma_q(\eta_1)\,\mathrm{d}\eta_1 \tag{51}$$

and normalize the axial separation η_1 with L_{xq}, we obtain with $\xi = \eta_1 / L_{xq}$

$$\psi = kL_{xq} \left(\frac{a_0}{U_p} + \frac{\cos\theta_e}{D_f} \right) \xi. \tag{52}$$

The nondimensional interference integral $F_q^\star$ according to equation (42) is then given by

$$F_q^\star = L_{xq}/D_j \int_{-\infty}^{\infty} \gamma_q \, \cos(\psi_q + \psi_r)\,\mathrm{d}\xi, \tag{53}$$

The phase speed U_p can be deduced from linear instability theory (Michalke & Hermann (1982)[17]), which yields frequency dependent values around

$$U_p = U_f + 0.7\,(U_j - U_f). \tag{54}$$

B. Mach wave radiation

Maximum sound emission of a source volume element according to equations (31) or (32) is achieved for the smallest possible values of ψ defined by equation (52). The phase ψ vanishes according to equation (52) for an emission angle

$$\cos\theta_{eM} = -\frac{a_0}{U_p - U_f}. \tag{55}$$

This condition can only occur if the relative phase speed $U_p - U_f$ of the jet is larger than the ambient speed of sound a_0,

$$\frac{U_p - U_f}{a_0} > 1. \tag{56}$$

The sound radiation into the angle defined by equation (55) is called Mach wave radiation. According to equation (54), the jet speed of a jet has to be at least 1.4 times the ambient speed of sound plus the flight speed for that to happen. For a given jet speed U_j, $U_j - U_f$ is smaller in flight than during static operation of the engine. This means that the Mach wave radiation angle θ_{eM} moves to the rear in flight. Mach wave radiation can even disappear in flight, which is the normal case for commercial aircraft in cruise.

The power-spectral density of the sound pressure in the far field for the Mach wave radiation angle is then given by

$$W_{ppqq}(x_i, f) = \left(\frac{\gamma p_0}{4\pi} \right)^2 \left(\frac{D_j}{r_e} \right)^2 \left(\frac{\Delta U_j}{a_0} \right)^7 \frac{\sigma}{D_f^6} \frac{L_{xq}}{D_j} \int_V W_{qqs}^\star \mathrm{d}V^\star(y_i). \tag{57}$$

It is noteworthy that the contribution of a volume element $\mathrm{d}V^\star(y_i)$ in the source region to the frequency spectrum in the far field is identical to the frequency spectrum in the source region. The source spectrum is not altered by interference effects because $F_q^\star = 1$ for Mach wave radiation.

Mach wave radiation is not restricted to small frequencies as claimed by Tam.[22] The fact that higher frequencies are not observed in the rear arc may have two causes. Firstly, the effects of wave refraction which were experimentally verified by Atvars et al.[24,25] are excluded in this simple model. They affect the spectral shape especially for high frequencies for angles close to the jet axis. Secondly, the interference in the radial direction is discarded in this simple model. The noise reduction through radial interference will necessarily be stronger when the wave length is small im comparison to the jet diameter. This can already be concluded from Michalke,[5,7] who already discussed the noise emission of instability waves.

It may be noted that this result shows that Mach wave radiation can be described with the acoustic analogy in contrast to the claim of Tam[22] and it exists for the quadrupole sources as well as for the dipole sources. The noise emission by instability waves is included in the solution for the geometric far field given by equation (27) for the quadrupole sources and equation (29) for the dipole sources.

C. Coherence models

Three different coherence models shall be investigated. For each of them a closed form solution exists for the interference integral

$$F_r = F_q^\star D_j / L_{xq} = \int_{-\infty}^{\infty} \gamma_q(\xi) \cos\left(2\pi \frac{f L_{xq}}{U_p} \left[1 + \frac{U_p}{a_0} \frac{\cos\theta_e}{D_f} \right] \xi \right) \mathrm{d}\xi. \tag{58}$$

Model 1 describes a coherence between two axially displaced positions in a nozzle-fixed coordinate system that decays exponentially with the normalized separation distance $\xi = \eta_1 / L_{xq}$ according to

$$\gamma = \exp(-2|\xi|). \tag{59}$$

The length scale L_{xq} is a function of frequency in this frequency dependent description. [a]

A second shape for the coherence function is given by

$$\gamma = \frac{1}{1 + \pi^2 \xi^2}. \tag{60}$$

The coherence of turbulent fluctuations in a frame moving with the flow is often modeled by the Gauss function. If we assume such a behavior in the nozzle-fixed coordinate system we have

$$\gamma = \exp(-\pi \xi^2). \tag{61}$$

The three coherence models are compared in figure 4. The coherence functions of models 2 and 3 have a gradient zero for $\xi = 0$. Model 3 has the widest distribution close to $\xi = 0$ but the most rapid decay for large separations ξ.

D. Interference integrals

The interference effect is the result of the interference integral of equation (58). Using the coherence model 1 of equation (59) we obtain the analytical solution

$$F_{r1} = \frac{1}{1 + [\pi (f L_{xq}/U_p)(1 + (U_p/a_0)\cos\theta_e/D_f)]^2}. \tag{62}$$

The integral based on coherence model 2 of equation (60) is

$$F_{r2} = \exp\left[-2 \frac{f L_{xq}}{U_p} \left| \left(1 + \frac{U_p}{a_0} \frac{\cos\theta_e}{D_f} \right) \right| \right] \tag{63}$$

and the interference integral with coherence model 3 of equation (61) is

$$F_{r3} = \exp\left[-\pi \left(\frac{f L_{xq}}{U_p} \left(1 + \frac{U_p}{a_0} \frac{\cos\theta_e}{D_f} \right) \right)^2 \right]. \tag{64}$$

[a] The turbulence length scale in numerical computations is defined differently in a moving frame of reference and as an integral value over the whole frequency range.

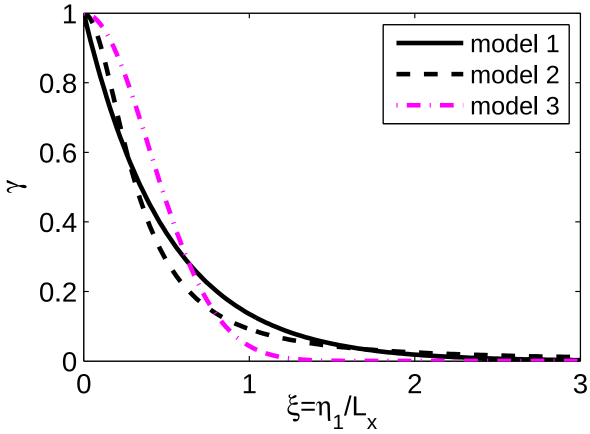

Figure 4. Comparison of the three investigated coherence models.

E. Influence of axial length scale

The influence of the Strouhal number fL_{xq}/U_p, which can be considered a normalized length scale, is studied first. The result for coherence model 1 and an acoustic Mach number of the convected turbulence $U_p/a_0 = 1.2$ and for the flight Mach number $M_f = 0$ is shown in figure 5(a) as a function of emission angle θ_e.

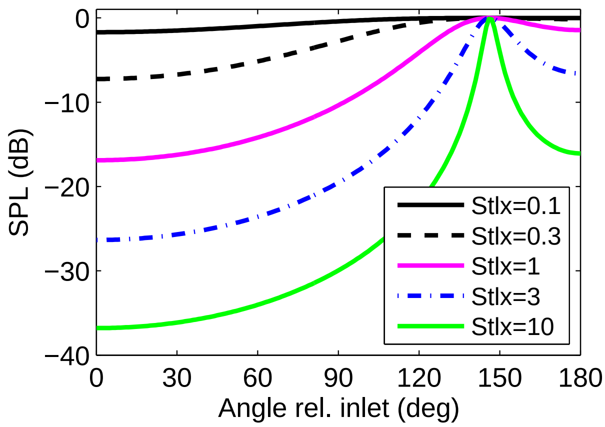

(a) $U_p/A_0 = 1.2$

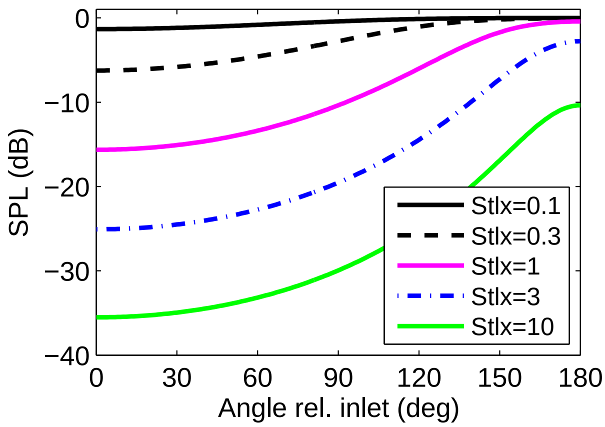

(b) $U_p/A_0 = 0.9$

Figure 5. Interference integral for various length scales fL_{xq}/U_p and two phase Mach numbers U_p/a_0 with coherence model 1. The maximum at $146°$ in the left figure is due to Mach wave radiation.

It can be seen that the convective amplification in the rear arc depends strongly on the length scale fL_{xq}/U_p of the source distribution in the turbulent flow field. The curves reach a value of 0 dB for the Mach wave radiation angle of $\theta_{eM} = 146°$. The directivity is reduced due to interference for all other angles, the effect increases with the length scale. The result for one value for fL_{xq}/U_p is valid for all frequencies if the product fL_{xq} remains constant for a constant phase speed U_p. This is the case if the length scale is proportional to the wave length of the generated sound.

The results for a subsonic phase speed $U_p/a_0 = 0.9$ are shown in figure 5(b). The directivities peak at $180°$ because the refraction dimple[24,25] in the rear arc due to wave refraction is not considered by this simple model.

The next two figures 6(a) and 6(b) describe the same results for the coherence model 2. It can be seen that the level reduction in the forward arc due to interference is much larger for coherence model 2 than for model 1.

The next two figures 7(a) and 7(b) describe the same results for the coherence model 3. The level reduction in the forward arc due to interference is even larger for coherence model 3. The reduction is unrealistically large. Therefore, model 3 will not be studied further because it is not applicable for the fixed frame of reference used here.

It can be concluded that convective amplification requires large coherence length scales in the streamwise direction. The experimentally observed convective amplifications are compatible with $fL_x/U_p \approx 1$. For a Strouhal number

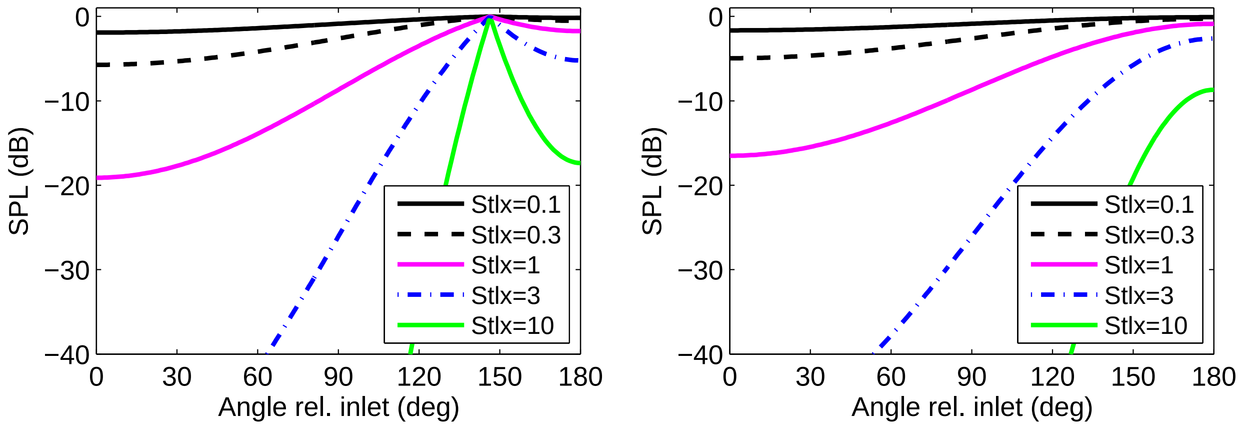

(a) $U_p/A_0 = 1.2$ (b) $U_p/A_0 = 0.9$

Figure 6. Interference integral for various length scales fL_{xq}/U_p and two phase Mach numbers U_p/a_0 with coherence model 2. The maximum at $146°$ in the left figure is due to Mach wave radiation.

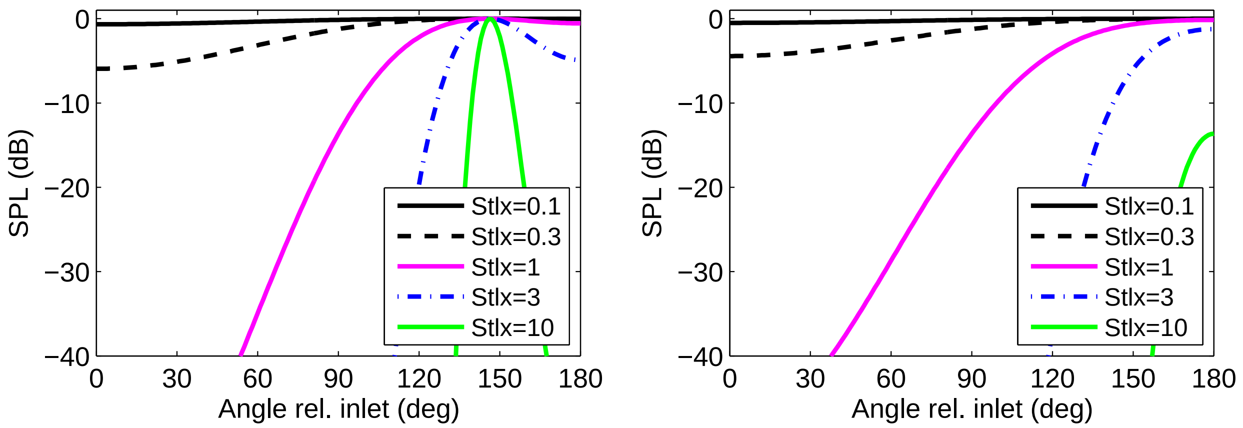

(a) $U_p/A_0 = 1.2$ (b) $U_p/A_0 = 0.9$

Figure 7. Interference integral for various length scales fL_{xq}/U_p and two phase Mach numbers U_p/a_0 with coherence model 3. The maximum at $146°$ in the left figure is due to Mach wave radiation.

$fD_j/U_j = 1.0$ (peak Strouhal number of one-third octave band spectra) and $U_p/U_j = 0.7$ the length scale is $L_x \approx 0.7D_j$.

F. Influence of axial phase speed

The influence of the acoustic phase Mach number $Ma_p = U_p/a_0$ is studied next for a length scale $fL_{xq}/U_p = 1$. The results for models 1 and 2 are shown in figures 8(a) and 8(b). The resulting directivity shapes are as expected, since the convective amplification in the rear arc increases with U_p/a_0. The spread between the curves in the forward arc is larger for model 2.

G. Influence of flight Mach number

The influence of the flight Mach number is studied now for the two coherence models. The phase speed $U_p/a_0 = 1.2$ and the length scale $fL_{xq}/U_p = 1$. The results are shown in figures 9(a) and 9(b). The Doppler amplification D_f^{-6} for the quadrupole sources (see equation (41)) is considered. The influences of the changed relative jet speed $U_j - U_f$, of the factor L_x/D_j in equation (53), and of a possible jet stretching in flight are not included. Therefore, the directivity values remain uninfluenced by Ma_f at $\theta_e = 90°$. Note that the chosen coherence model has a large influence on the sound radiation into the forward arc.

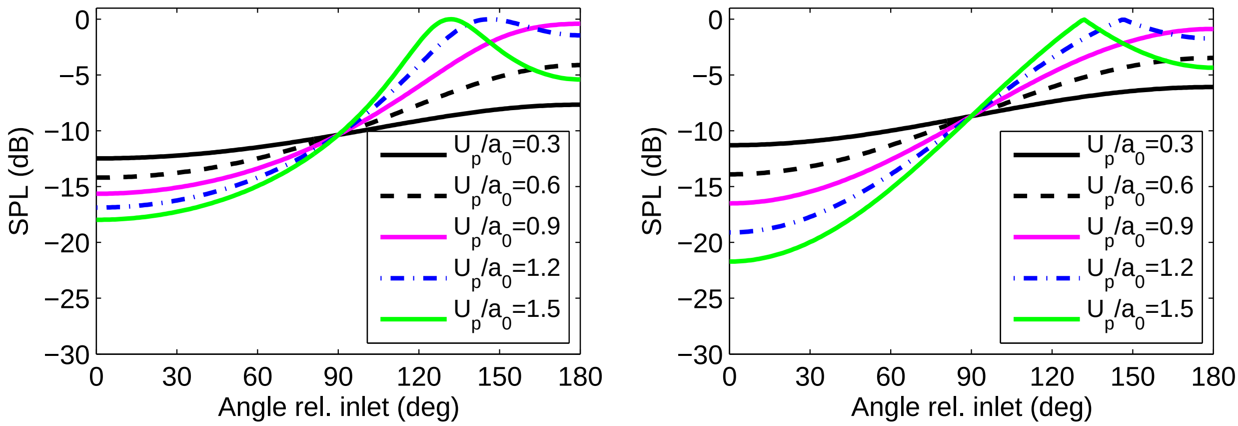

(a) Model 1 (b) Model 2

Figure 8. Interference integral for various phase Mach numbers U_p/a_0 and $fL_{xq}/U_p = 1$.

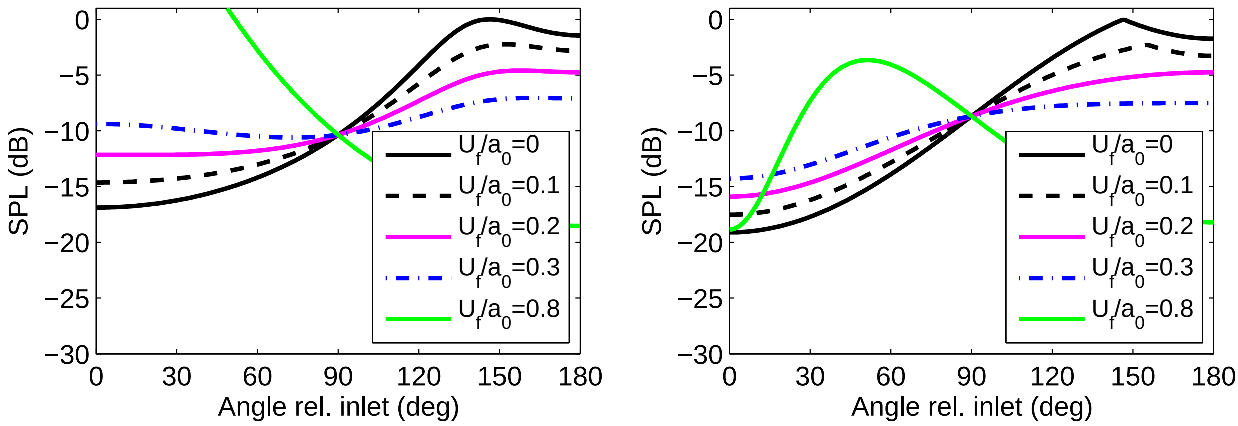

(a) Model 1 (b) Model 2

Figure 9. Interference integral for various flight Mach numbers U_f/a_0 with $fL_{xq}/U_p = 1$ and $U_p/a_0 = 1.2$. Doppler amplification D_f^{-6} for quadrupole sources included. The radiation into the forward arc, escpecially at cruise Mach numbers depends strongly on the chosen coherence model. The actual behavior of a jet in cruise cannot be derived, but a high noise emission into the forward arc cannot surprise.

The forward arc amplification becomes very strong for flight Mach numbers during cruise but depends considerably on the chosen coherence model. The actual behavior of a jet in cruise cannot be predicted with this simple model but a high noise emission into the forward arc cannot surprise. Since the jet is stretched substantially at cruise Mach numbers, the low frequency jet sources are located much farther downstream than in a static condition. The consequence is that the cabin of an aircraft may be located in the main beam of jet mixing noise during cruise.

The results for dipole sources, where the Doppler amplification is D_f^{-4} are shown in figures 10(a) and 10(b). The forward arc amplification is slightly smaller.

H. Influence of acoustic jet Mach number

The influence of the acoustic jet Mach number U_j/a_0 is shown in figure 11(a) for the coherence model 1 and in figure 11(b) for coherence model 2. for three emission angles $\theta_e = 60°, 90°, 120°$. The flight Mach number $M_f = 0$. Lighthill's result of $\overline{p^2} \propto (U_j/a_0)^8$ for an emission angle of $\theta_e = 90°$ is recovered.

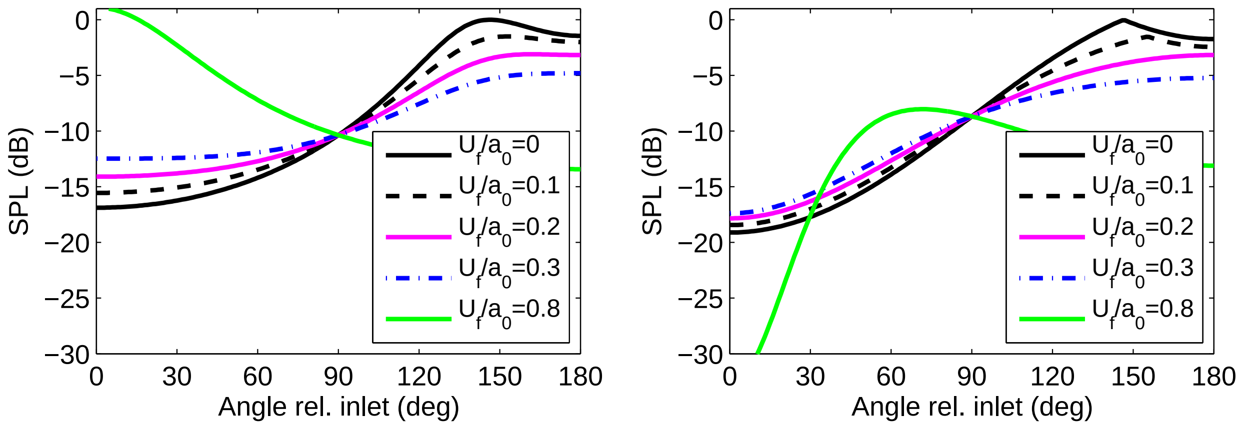

(a) Model 1 (b) Model 2

Figure 10. Interference integral for various flight Mach numbers U_f/a_0 with $fL_{xq}/U_p = 1$ and $U_p/a_0 = 1.2$. Doppler amplification D_f^{-4} for quadrupole sources included. The radiation into the forward arc, escpecially at cruise Mach numbers depends strongly on the chosen coherence model.

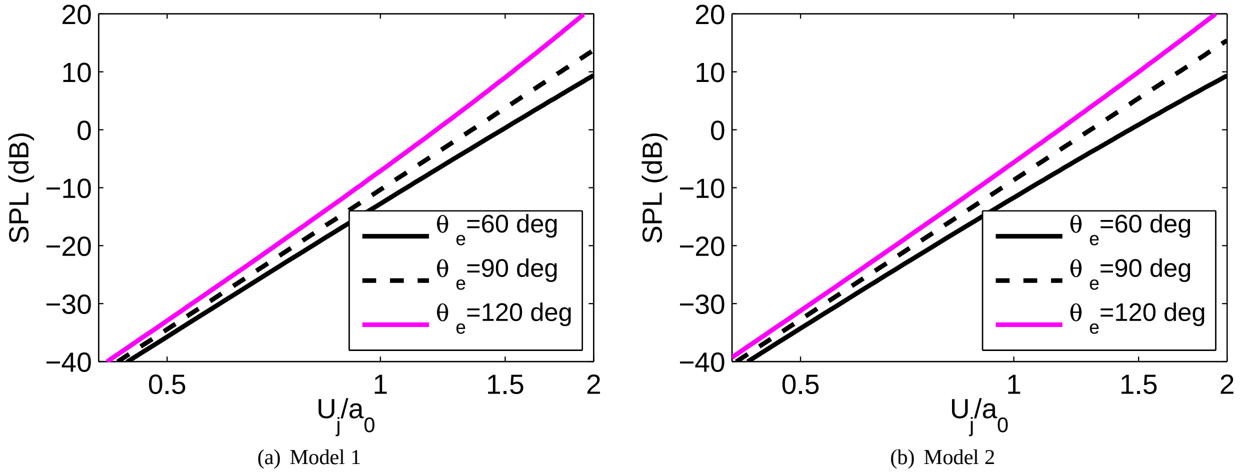

(a) Model 1 (b) Model 2

Figure 11. Influence of acoustic jet Mach number U_j/a_0 and emission angle θ_e on the sound radiation in a one-third octave band for $fL_{xq}/U_p = 1$ and a flight Mach number of $U_f/a_0 = 0$. The results for 90° agree with Lighthill's result of $\overline{p^2} \propto (U_j/a_0)^8$.

IV. Conclusions

The sound radiation of a free jet is studied in the frequency domain. An integral for the power-spectral density is derived, which includes the quadrupole sources for jets with constant mean density and the additional dipole sources of jets with nonuniform density. In contrast to the theories of Lighthill,[1,2] Ffowcs Williams,[3] and many others, the analysis is performed in a coordinate system fixed on the nozzle of the jet, where the source terms satisfy the mathematically important condition of stationary randomness and the limits of the source integral are stationary. Turbulence convection is considered through a phase angle of the cross-spectral density of the sources. The influence of source interference is expressed in terms of an interference integral which describes the sound radiation of one source volume element including the interference effects with its neighborhood.

In order to achieve analytic solutions for this integral, the radial extension of the jet is neglected and simple models are introduced for the decay of the coherence with increasing axial separation of the source positions. The interference effects reduce the sound emission for all angles except for the Mach wave radiation angle. Some main features of jet mixing noise can be explained with this simple model, the convective amplification, the Mach wave radiation and the independence of frequency with emission angle.

However, the model is admittedly crude. The neglect of the radial extension of the jet may be an acceptable approximation for long wave lengths, but it is certainly not valid for short wave lengths. The radial extension can be approximately considered when the source region is modeled by a cylindrical source distribution. This allows to decompose the cross-spectral density into azimuthal components according to Michalke[6] and a separate treatment of each component. The effect of radial interference should be largest in the case of Mach wave radiation where the low frequencies suffer no attenuation due to interference, while the attenuation due to radial interference is not negligible for higher frequencies. Also neglected are the effects of wave refraction which affect the radiation into the rear arc.

The results are

- The frequency in the far field is independent of source motion.
- The spectral shape is determined by interference effects, which are a function of frequency.
- The convective amplification in the rear arc depends on the axial length scale of the turbulence.
- Length scales in the order of one jet diameter are required to explain the measured convective amplification for the peak frequency of jet mixing noise.
- The coherence needs to decay rather rapidly in the axial direction for small separation distances in order to explain the experimentally observed directivities.
- The Gauss function is not a suitable assumption to describe the axial decay of coherence between two source positions in a nozzle fixed coordinate system.
- The Mach wave radiation for supersonic convection speeds is correctly described.
- The separation between jet noise from large scale turbulence and small scale turbulence found in the literature might be explainable as jet noise radiation with small source interference and large source interference effects.
- The flight speed yields a convective amplification of jet noise in the forward arc. The actual amplification depends strongly on the chosen coherence model.
- Jet noise should peak in the forward arc for cruise Mach numbers according to the results of the interference integral.
- The integral describing the noise emission of one volume element must be independent of the source definition, i.e., it should be applicable to the pseudo sound and the vortex sound source terms for low Mach number jets.
- The result for the noise emission of one volume element might be suitable for post-processing numerical simulation results.
- The result for the noise emission of one volume element might also help develop improved source localization procedures for the analysis of jet mixing noise on engine test beds.

Acknowledgments

The work was co-financed by the German Federal Ministry of Economics and Technology within the research project LEXMOS (Quiet nozzle systems and sound source localization).

References

[1] Lighthill, M. J., "On Sound Generated Aerodynamically. I. General Theory," *Proc. Roy. Soc. London*, Vol. A 211, 1952, pp. 564–587.

[2] Lighthill, M. J., "On Sound Generated Aerodynamically. II. Turbulence as a Source of Sound," *Proc. Roy. Soc. London*, Vol. A 222, 1954, pp. 1–32.

[3] Ffowcs Williams, J. E., "The Noise from Turbulence Convected at High Speed," *Phil. Trans. Roy. Soc.*, Vol. A 225, 1963, pp. 469–503.

[4] Ribner, H. S., "New Theory of Jet-Noise Generation, Directionality, and Spectra," *J. Acoust. Soc. Am.*, Vol. 31, 1959, pp. 245–246.

[5] Michalke, A., "A Wave Model for Sound Generation in Circular Jets," Deutsche Luft- und Raumfahrt, DLR FB 70-57, 1970.

[6] Michalke, A., "An Expansion Scheme for the Noise From Circular Jets," *Z. Flugwiss.*, Vol. 20, 1972, pp. 229–237.

[7] Michalke, A., "On the Effect of Spatial Source Coherence on the Radiation of Jet Noise," *J. Sound Vib.*, Vol. 55, 1977, pp. 377–394.

[8] Michalke, A., "Some Remarks on Source Coherence Affecting Jet Noise," *J. Sound Vib.*, Vol. 87, 1983, pp. 1–17.

[9] Michalke, A. and Michel, U., "Prediction of Jet-Noise in Flight from Static Tests," *J. Sound Vib.*, Vol. 67, 1979, pp. 341–367.

[10] Michalke, A. and Michel, U., "Importance of Jet Temperature on the Prediction of Jet-Noise in Flight," *Mechanics of Sound Generation in Flows*, edited by E.-A. Müller, Springer-Verlag Berlin Heidelberg, 1979, pp. 256–263, Proceedings of the IUTAM/ICA/AIAA-Symposium, Göttingen, August 28-31, 1979.

[11] Michel, U. and Michalke, A., "Prediction of Flyover Jet Noise Spectra," AIAA Paper 81-2025, 1981, AIAA 7th Aeroacoustics Conference.

[12] Michel, U. and Michalke, A., "Prediction of Flyover Jet Noise Spectra From Static Tests," NASA Technical Memorandum 83219, 1981.

[13] Michel, U., "Broadband Shock Noise: Theory Vis-A-Vis Experimental Results," *First Joint CEAS/AIAA Aeroacoustics Conference (16th AIAA Aeroacoustics Conference)*, 1995, pp. 545 – 554, CEAS/AIAA Paper 95-071, DGLR-Bericht 95-01.

[14] Tam, C. K. W. and Auriault, L., "Jet Mixing Noise from Fine-Scale Turbulence," *AIAA J.*, Vol. 37, 1999, pp. 145–153.

[15] Ffowcs Williams, J. E., "Hydrodynamic Noise," *Annual Review of Fluid Mechanics*, Vol. 1, 1969, pp. 197–222.

[16] Morfey, C. L., "Amplification of Aerodynamic Noise by Convected Flow Inhomogeneities," *J. Sound Vib.*, Vol. 31, 1973, pp. 391–397.

[17] Michalke, A. and Hermann, C., "On the Inviscid Instability of a Circular Jet With External Flow," *J. Fluid Mech.*, Vol. 114, 1982, pp. 343–359.

[18] Ribner, H. S., "Aerodynamic Sound from Fluid Dilatations, A Theory of the Sound from Jets and other Flows," Report 86, Institute of Aerophysics, University of Toronto, 1962.

[19] Powell, A., "Theory of Vortex Sound," *J. Acoust. Soc. Am.*, Vol. 36, 1964, pp. 177–195.

[20] Möhring, W., "On Vortex Sound at Low Mach Number," *J. Fluid Mech.*, Vol. 85, 1978, pp. 685–691.

[21] Obermeier, F., "On a New Representation of Aeroacoustic Source Distribution. I: General Theory. II: Two-dimensional Model Flows." *Acustica*, Vol. 42, 1979, pp. 56.

[22] Tam, C. K. W., "Computational Aeroacoustics Examples Showing the Failure of the Acoustic Analogy Theory to Identify the Correct Noise Sources," *J. Comp. Acoustics*, Vol. 10, 2002, pp. 387–405.

[23] Maestrello, L., "Statistical Properties of the Sound and Source Fields of an Axisymmetric Jet," AIAA Paper 77-1267, 1977, AIAA 4th Aeroacoustics Conference.

[24] Atvars, J., Schubert, L. K., and Ribner, H. S., "Refraction of Sound from a Point Source Placed in an Air Jet," *J. Acoust. Soc. Am.*, Vol. 37, 1965, pp. 168.

[25] Atvars, J., Schubert, L. K., Grande, E., and Ribner, H. S., "Refraction of Sound by Jet Flow or Jet Temperature," TN 109 (1965); NASA CR-494 (1966), University of Toronto, Institute for Aerospace Studies, 1965.